

An Investigation of Solutions of Sulfur in Oleylamine by Raman Spectroscopy and Their Relation to Lead Sulfide Quantum Dot Synthesis

Thesis Written By: Michael Lynch, Department of Chemistry and Biochemistry

Thesis Defense Date: April 10th, 2017

Thesis Advisor: Dr. David Jonas, Department of Chemistry and Biochemistry

Honors Council Representative: Dr. Robert Parson, Department of Chemistry and Biochemistry

Additional Committee Members: Dr. Chuck Rogers, Department of Physics

Abstract

The first Raman spectrum of oleylamine was obtained after a multistep purification procedure based on acid-base chemical exchange techniques. The purification was needed because commercially available oleylamine shows photoluminescence in the Raman spectrum, obscuring the Raman peaks. Using the purified oleylamine, sulfur in oleylamine solutions were studied by resonance Raman, UV-vis, absorbance, NMR, and IR spectroscopy. Additionally, the time dependence of sulfur species present in these solutions was studied over several days using Raman spectroscopy. Based on the changes in the Raman spectra over time, it is hypothesized that the concentration of the polysulfide species S_4^{2-} increases, while the polysulfide species S_6^{2-} decreases over time in solutions of sulfur in oleylamine. Based on UV-vis spectra of lead sulfide quantum dots synthesized with sulfur in oleylamine precursor that was aged for different times, it is suggested that when a solution of sulfur in oleylamine is used as a precursor for the synthesis of lead sulfide quantum dots, it is best used within a few hours of preparation in order to minimize the absorption linewidth of the quantum dot 1S-1S transition (the lowest lying electronic transition). Spectroscopic information about the sulfur species present in sulfur oleylamine solutions during the first few hours and at later times is further discussed.

Introduction

Sulfur in amine solvents has been of interest to chemists since 1921 due to applications such as accelerating the vulcanization process¹⁻⁴, producing deep beautiful colors,⁵ and understanding the color of Ultramarine paints.⁶⁻⁸ Today the study of sulfur in amine solvents is important for quantum dot (QD) synthesis and, more generally, nanomaterial synthesis. QDs are nanocrystalline semiconductors whose size is on the order of the Bohr-exciton radius. At these nanometer and smaller sized scales, quantum effects become manifest. The most remarkable aspect of QDs is that their size is easily tunable, allowing one to fine-tune the wavelength of light they absorb. The nature of the active sulfur-species responsible for nanocrystal growth in solutions of sulfur in amine solvents, particularly sulfur in oleylamine (OIAM), is not known. The reactions of sulfur in OIAM are interesting, in part, because there are many past studies of the reactions of olefins with sulfur and many studies of the reactivity of amines with sulfur, but there are comparatively few studies on the reactivity of sulfur with olefinic amines, of which OIAM is an example (Figure 1). OIAM is useful in nanocrystal synthesis due to its ability to simultaneously act as a solvent (it's a liquid a room temperature), surfactant, and a reducing agent. Additionally, commercial OIAM is relatively cheap compared to other reagents one might use for nanocrystal synthesis.⁹ This study focused on the nature of the sulfur species responsible for lead sulfide (PbS) synthesis for the purposes of improving metal sulfide nanomaterial syntheses that involve sulfur in oleylamine as a precursor. Examples of metal sulfide nanomaterial syntheses that use this precursor are Ag₂S nanocrystals, Cu₂S nanoplates, CdS nanorods, and many more.⁹

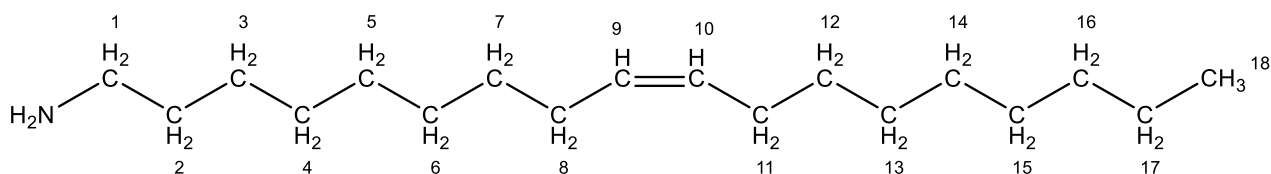


Figure 1: Molecular structure of oleylamine. The numbers at each position refers to the carbon atom number. The double bond is between carbons 9 and 10. Typically, in a hydrocarbon molecular structure the carbon atoms represented as vertices with the number of hydrogens attached implied (so that the valence of carbon adds to four).

One synthesis of PbS QDs is based on a reaction between lead (II) chloride in OIAM and a solution of sulfur in OIAM (S-OIAM).¹⁰ A solution of S-OIAM is bright yellow or orange in color and its optical absorption spectrum changes over time. The synthesis appears to produce high quality PbS nanocrystals with one sharp peak in the absorption spectrum when fresh S-OIAM solution is used for the synthesis; when aged S-OIAM is used, the synthesis gives a broader peak, which is typically undesirable because it correlates to a broader size distribution of QDs. PbS nanocrystals with two peaks around the 1S-1S transition in their absorption spectrum have been observed when using aged sulfur-amine solutions for synthesis.¹¹ We hypothesize that this might be due to undesirable sulfide species being more stable in the oleylamine than the more desirable sulfide species, which is short lived in oleylamine.

Elemental sulfur exists at normal temperatures and pressures as a yellow solid in the form of an eight-membered cyclic ring, S_8 . Sulfur is known to exist in the form of polysulfides, multiatom linear chains of sulfur atoms, both anionic and cationic, all the way from 2 atoms in a chain to over 8 atoms in length (Figure 2).¹² Sulfur dissolved in electron pair donating solvents, such as amines, has been observed in the form of anionic polysulfides.

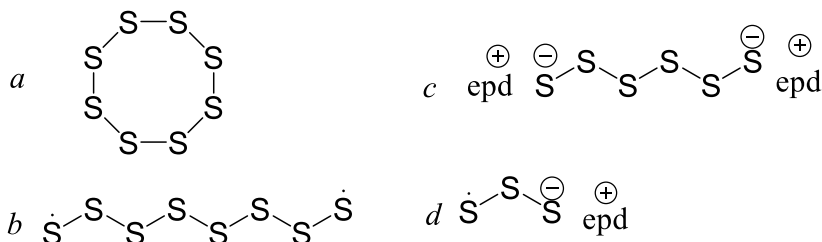


Figure 2: Various forms of sulfur. epd- Electron Pair Donating solvent. a: Cyclic S_8 , b: Linear S_8 , c: S_6^{2-} , d: S_3^-

Evidence from electron spin resonance¹³, conductivity⁵, and electrophoresis¹⁴ studies suggests elemental sulfur dissolved in amines will form radical anions and other negatively charged sulfur species. These solutions are often brightly colored and their color changes with time.⁵ Davis and Nakshbendi classify solutions of sulfur in amines into three different classes based on the structure of the amine.⁵ Solutions of sulfur in tertiary amines change color slowly, while solutions of secondary amines change somewhat faster, and solutions of primary amines change fastest. Common polysulfides observed in these solutions are S_2^- , S_3^- , S_4^- , S_4^{2-} and S_6^{2-} .^{7,13,15-17} S_3^- is well characterized by electrical transference, conductivity, magnetic susceptibility, quantitative spectrophotometric titration and spectroscopy as the species responsible for blue solutions of sulfur in the electron pair donating solvents hexamethylphosphoramide (HMPA) and dimethylformamide (DMF).¹⁸⁻²⁰ The other polysulfide species are not as well characterized. Resonance Raman spectroscopy has been a method of choice to characterize polysulfide species in solution, as pioneered by works of T. Chivers²¹ and R.J. Clark's⁷ groups. Other analytical methods such as NMR and mass-spectroscopy, among others, have not been proven useful in observation of polysulfides.²²

Raman spectroscopy is a form of vibrational spectroscopy that is used (typically along with IR spectroscopy) to elucidate information about molecular structure. Raman scattering occurs when light is inelastically scattered from a molecule. The term “inelastic” means the final (scattered) photon has a different energy than the initial photon. If the photon is scattered with more energy, the scattering is anti-Stokes Raman scattering. If the photon is scattered with less energy than the incident photon, the scattering is called Stokes Raman scattering. Raman scattering is different from Rayleigh scattering, which occurs when light is elastically scattered or, in other words, when the final photon has the same energy as the initial photon. Scattering is sometimes thought of as proceeding through a “virtual” excited state followed by emission back to the ground state, where the final vibrational state may (Rayleigh scattering) or may not (Raman scattering) be the same as the initial vibrational state. The origin of Raman scattering involves the interaction of the incident electromagnetic wave with electromagnetic field produced by a molecule or atom. For a normal mode of a molecule or atom to be “Raman active” its polarizability must change during that normal mode's vibration. The polarizability of a molecule is a measure of how easily the electron cloud is distorted. For example, as you go down a column of the periodic table the atoms have higher polarizability.²³

The Raman effect should not be confused with fluorescence. In fluorescence spectroscopy, an atom or molecule absorbs an incident photon which promotes the molecule to an (actual) excited electronic state. From the excited electronic state the photon is emitted, usually with lower energy due to non-radiative vibrational decay.²⁴ Because there are many vibrational levels to decay to, fluorescence bands are much broader than Raman bands. Unlike fluorescence spectroscopy, Raman spectroscopy can be performed at any wavelength, the photons will always be scattered in the same manner, and the Raman peaks will always be the same difference in energy away from the incident photon. An illustration of the fluorescence and Raman processes are shown in Figure 3. A common problem in Raman spectroscopy is the obscuration of the spectrum due to photoluminescence (fluorescence or phosphorescence) which may be caused by impurities in the sample.²³ One can change the incident wavelength in order to decrease photoluminescence due to impurities. Alternatively, one can purify the sample to obtain a clean Raman spectrum.

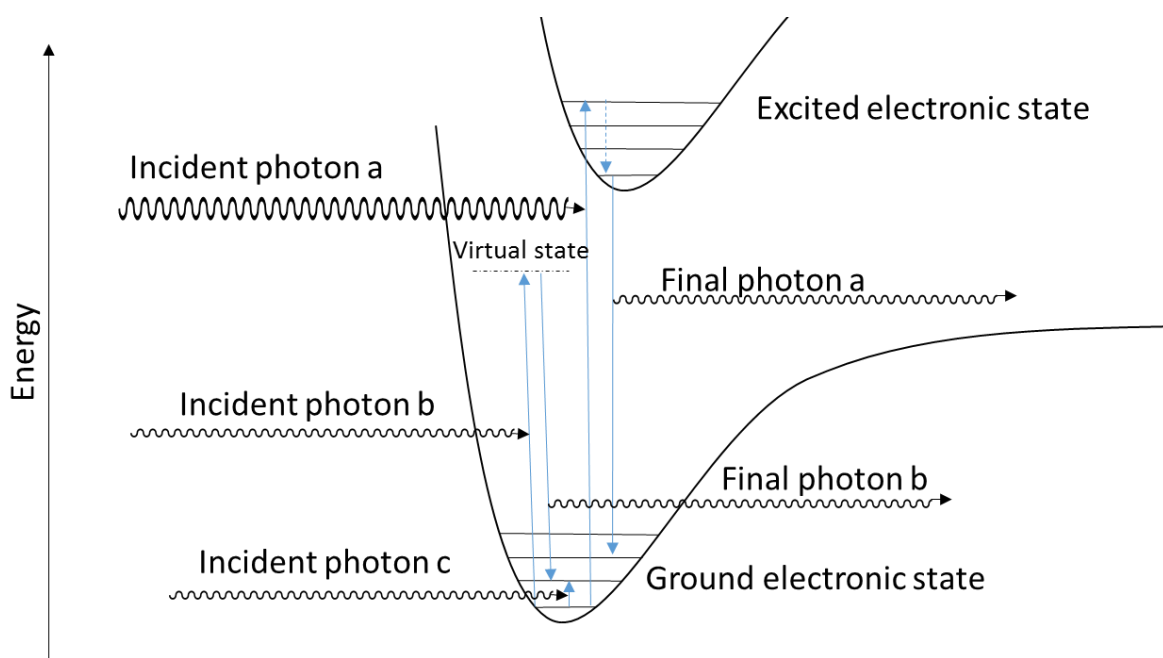


Figure 3: Diagram showing IR absorption, Raman, and fluorescence processes. Vibrational states are represented by horizontal black lines within the electronic state potentials (only a few are shown). Fluorescence is illustrated by absorption of 'incident photon a' followed by vibrational relaxation before emission of 'final photon a'. The dotted blue arrow in the excited electronic state represents vibrational decay. Raman scattering is illustrated by absorption of 'incident photon b' to a virtual state followed by emission of 'final photon b' (Stokes scattering). IR absorption is illustrated by absorption of 'incident photon c'.

Resonance Raman spectroscopy is a variation of Raman spectroscopy allowing enhanced Raman scattering signal from light absorbing species in the sample. In resonance Raman, the incident wavelength is close to an electronic transition energy of the absorbing species which results in more intense Raman scattering.²⁵ In other words, in resonance Raman the "virtual" excited state becomes very close in energy to the (actual) excited state. As mentioned above, resonance Raman has been performed extensively to characterize the various polysulfide species. Table 1 gives a summary of the literature assignments of Raman shifts, UV-Vis absorption, and IR absorption for various polysulfide species.

The active sulfur species responsible for initiating the nucleation burst to form PbS nanocrystals is unknown although there is some speculation from recent studies coming to various conclusions. It has been known since 1962 that sulfur reacts with secondary amines to produce the respective thioamide (R-(C=S)-NH₂) and hydrogen sulfide.³⁰ Thomson et al. studied the reaction of sulfur in octylamine, a molecule that closely resembles oleylamine, but has no double bond and only an 8 carbon chain. They reported that at low temperatures alkylammonium polysulfides are formed based on ¹H NMR evidence that showed a linear downfield shift of the amine proton's peak and a linear decrease in the diffusion coefficient as the solution became more concentrated. They reported that at high temperatures (130 °C), organosulfur compounds formed include octanethioamide, N'-octyloctanamide, and α-thioketoamidine (Figure 4a). They propose these are intermediates which react further to give hydrogen sulfide which reacts with the metal to form the QD.³¹ McPhail and Weiss studied the reaction of sulfur in 1-octadecene (ODE), another molecule which resembles oleylamine, but has no amine group and has a terminal double bond instead of an internal double bond. They report that at high temperatures hydrogen sulfide is formed and organosulfur compounds are formed of which the products are a sulfur chain terminally bound to a saturated alkane and a sulfur chain terminally bound to a hydrocarbon chain with an internally migrated double bond (Figure 4b).³² Moore and Saville have concluded the reaction of diethylamine and sulfur produce N-ethylthioacetamide as the major product, NN-diethylthioacetamide and diethylammonium hydrogen sulfide as minor products. When cyclohexene is added the same products are produced as well as cyclohexane rings connected with 1 or 2 S atoms (Figure 4c).³ Additionally, Moore and Saville have stated amines and sulfur react to produce hydrogen sulfide which reacts with cyclohexene. They report diethylamine and sulfur react with trisubstituted alkenes to produce tertiary-alkanethiols and di-tertiary-alkyl disulphides (Figure 4d).²

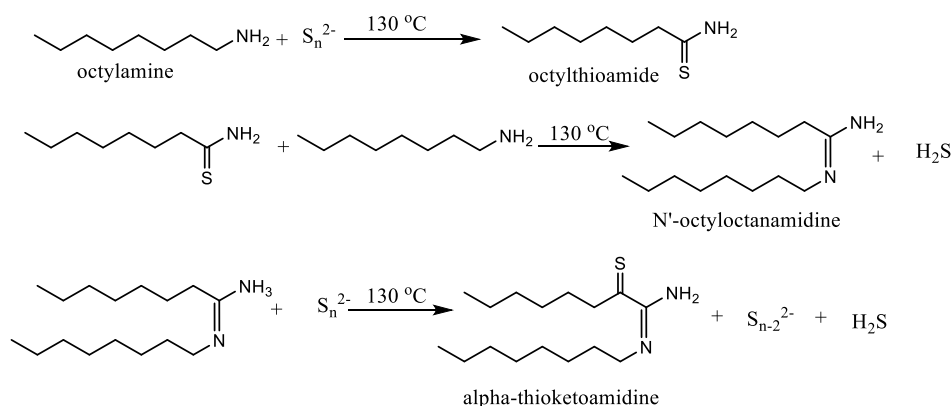


Figure 4a: Reactions of sulfur in octylamine from Thomson et. al. They suggest sulfur is present in octylamine as a polysulfide species which they represent as S_n²⁻.

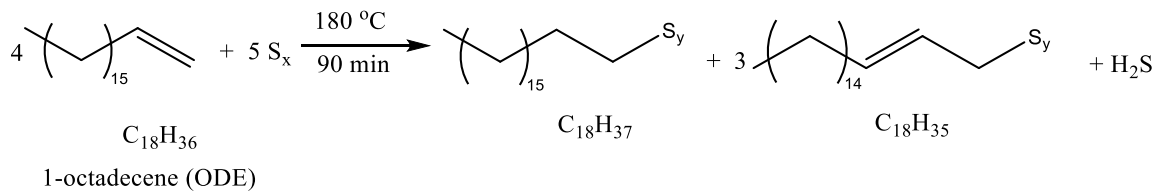


Figure 4b: Reactions of sulfur in ODE from McPhail and Weiss. They suggest sulfur is present as a radical or anionic polysulfide chain (S_x , where x equals the number of sulfur atoms in a chain). The double bond in the second product is shown between carbons 2 and 3, but can migrate to other internal positions. The subscript “ y ” on “ S_y ” equals $x-1$ or x . The chemical formulas are shown for easy calculation of the change in number of H atoms.

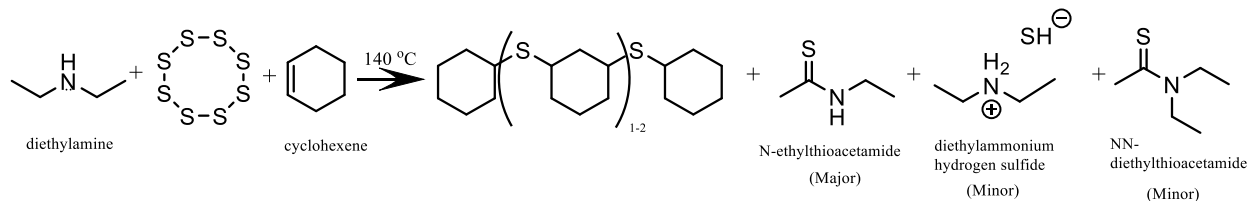


Figure 4c: Reactions from Moore et al. Part 1. Reaction of diethylamine and sulfur produces the very right three products when they react with themselves and produce the same three products plus cyclohexane connected with 1 or 2 S atoms when they react with cyclohexene.

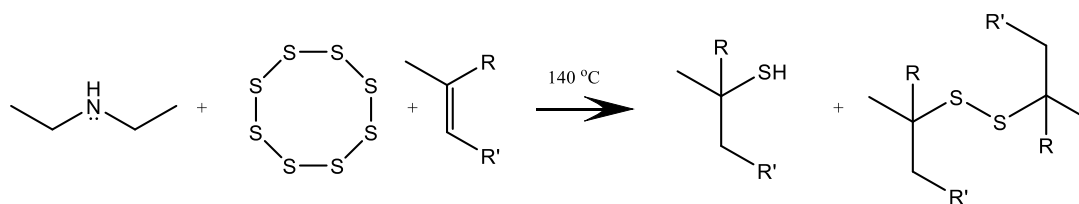


Figure 4d: Reaction from Moore et al. Part 2. The reaction of diethylamine, sulfur and a trisubstituted alkene produces thiols and disulfides. “R” and “R’” represent any alkyl group.

Davis and Nakshbendi state that the most common reaction of elemental sulfur with aliphatic amines is oxidation of the alpha carbon (carbon adjacent to nitrogen) and production of hydrogen sulfide.⁵ They conclude that alkylammonium polysulfide salts are formed from their studies on the conductance of amine sulfur solutions, which show that these solutions are highly conductive. Based on Davis and Nakshbendi’s work, we can consider the mechanism of the production of alkylammonium polysulfides as two steps. This basis rests on the assumption that primary amines have similar reactivity to secondary amines. First, is the ring breakage where the eight-membered ring of sulfur undergoes a nucleophilic attack by the lone pair on the oleylamine nitrogen (see Figure 5) to form an anionic linear polysulfide chain covalently bound to a positively charged nitrogen. Second, since there is a large excess of amine (the solvent), salt formation happens by the exchange of a proton between amine molecules to form the oleylammonium polysulfide salt. The mechanism is reversible as evidenced by the observation that the elemental sulfur can be quantitatively recovered by addition of a strong acid.⁵

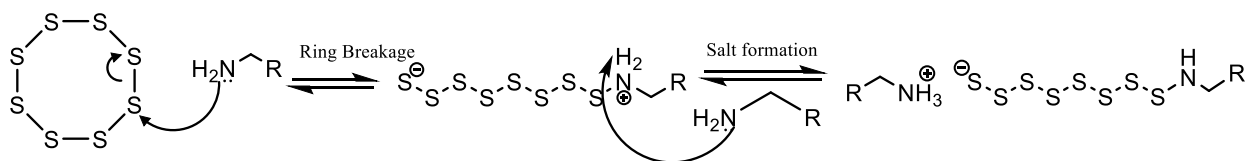


Figure 5: Proposed mechanism for the formation of oleylammonium polysulfide salt. “R” represents the part of the OIAm molecule not shown.

Previous resonance Raman studies have shown that the concentration of different polysulfide species dissolved in amines changes over time.^{33,34} The present work adds to the body of knowledge about sulfur in amine solvents with the study of elemental sulfur dissolved in oleylamine. Notably, this is the first study of elemental sulfur in OIAm solutions by Raman spectroscopy. Aldrich supplied oleylamine contains impurities which produce photoluminescence under 488 and 532 nm light, obscuring the Raman spectrum. An industrial purification method was found to purify oleylamine³⁵ to the point where it was possible to take a Raman spectrum with little to no photoluminescence.

It was observed that when elemental sulfur is added to the purified oleylamine the Raman spectrum is still observable, although upon heating to 120 °C for 20 minutes or more, the spectrum once again becomes obscure due to photoluminescence, although the photoluminescence may be of a different nature. In addition to Raman, we used the methods of NMR (¹H and ¹³C), UV-Vis absorbance, and IR spectroscopy to study sulfur in oleylamine solutions.

Nanocrystal synthesis was done with a solution of “fresh” sulfur oleylamine precursor and “aged” sulfur oleylamine precursor. Specifically, the “fresh” precursor refers to a solution that was aged between 0 and 2 hours from the time the elemental sulfur came into contact with the oleylamine. The “aged” precursor refers to a solution that had been aged for approximately 48 hours. The differences in the nanocrystals from both solutions are discussed below.

Methods

Summary of Oleylamine purification procedure:

For a more detailed procedure see the appendix. To a 500 mL round bottom flask was added 50 mL of oleylamine (CAS# 112-90-3, Aldrich, ≥98% (primary amine), cat. no. HT-OA100-1.5KG), 160 mL of diethyl ether (BDH1121-1LPC, stabilized with 1 ppm of BHT, ACS grade, 1L, BDH), and a Teflon magnetic stirbar. While stirring, 15.5 mL of concentrated HCl (H613-05, 36.5%-38%, ACS Reagent grade, Macron Chemicals) was added dropwise to the solution over a period of 10 minutes, converting oleylamine to oleylammonium chloride. Into a 1000 mL Erlenmeyer flask was added 500 mL of acetonitrile (A21-1, Certified ACS, 1L, Fisher Scientific) followed by dropwise addition of the oleylammonium chloride-ether solution. Upon mixing of the oleylammonium chloride-ether solution with the acetonitrile a white precipitate was formed. After all the oleylammonium chloride-ether solution had been added, the mixture was immersed in an ice bath for 30 minutes. The mixture was passed through a Büchner funnel under reduced pressure. The solid collected in the funnel was rinsed four times with 100 mL portions of acetonitrile. Next, a resulting snowy white fluffy solid was put into a 500 mL round bottom flask and dried under vacuum for 30 minutes. After drying the solid, 200 mL of ether, and a magnetic stirbar were added. While this white slurry was being stirred, a solution of 12.3 grams of sodium hydroxide (S318-500, Certified ACS, Fisher Scientific) in 150 mL of DI water was prepared and added in small

portions, creating a two-phase mixture. The mixture was transferred into a separatory funnel and the organic phase was collected after being washed four times with 50 mL of DI water per wash. To the organic phase was added anhydrous sodium sulfate (S421-500, anhydrous, Certified ACS, Fisher Scientific) and the solution left to dry overnight. The next day, the solvent was evaporated and the final product was vacuum distilled over sodium to yield ~40 mL oleylamine. The oleylamine purified in this way is referred to as “purified oleylamine” in this work.

Summary of PbS Nanocrystal synthesis:³⁴

A solution of sulfur in oleylamine was prepared by combining a pre-weighed amount of powdered elemental sulfur (CAS# 7704-34-9, STREM, 99.999%, cat. no. 93-1616) with oleylamine (purified by procedure above) to make 2.3-2.5 mL of 6 mg/mL sulfur-oleylamine solution in a 4 mL glass vial capped with a Teflon-lined plastic cap. The combination was performed inside a glovebox under nitrogen atmosphere. For a PbS nanocrystal synthesis utilizing “fresh” S-OIAM solution, 2 ml of S-OIAM were used within 30 minutes of mixing sulfur and oleylamine (sulfur dissolves in ~10 minutes under shaking or stirring at 34 °C temperature of the glovebox atmosphere). Inside the glovebox, a solution of lead (II) chloride (PbCl₂) and oleylamine was prepared by mixing ~0.85 g of lead chloride (CAS# 7758-95-4, Alfa Aesar, ultra dry, 99.999%, cat. no. 42841) with 7.5 mL of oleylamine (purified by procedure above) in a round bottom flask equipped with a magnetic stirring bar. The flask was sealed with a rubber septum inside the glovebox, transferred into the fume hood, immersed into an oil bath that was heated from 19 °C to 117 °C over a period of 38 minutes, and placed under vacuum while being stirred. At this point all the PbCl₂ had dissolved and the flask was filled with N₂ and cooled to 40 °C – the temperature of the PbS nanocrystal synthesis. To the solution of lead chloride, 2 mL of sulfur-oleylamine solution was injected with a syringe, at which point the mixture turned to a dark brown within 5 seconds. The reaction mixture was kept stirring for 10 minutes, then 12 mL of anhydrous toluene (Aldrich, anhydrous, 99.8%, Sure/Seal™, ≤0.001% H₂O by manufacturer’s specification, 1L) was injected into the mixture. The reaction flask was then removed from the oil bath and immersed into an ice bath. Once the reaction mixture had cooled the washing procedure was performed in the following manner in a nitrogen gas filled glovebox. Within an hour of the nanocrystal synthesis, the reaction flask was transferred into the glovebox and divided equally into three centrifuge tubes. The centrifuge tubes were sealed and centrifuged at 3000 rpm for 3 minutes. After centrifugation, the supernatant was decanted into a new set of centrifuge tubes. To each new centrifuge tube was added 0.5 mL of acetonitrile (CAS# 75-05-8, Acros Organics, 99.9+%, Extra Dry, AcroSeal®, cat. no. 326810010) followed by vigorous manual shaking. The tubes were then centrifuged once more and the supernatant was discarded. To the precipitate was added 5 mL of toluene and the tube was vigorously shaken manually. Ligand exchange was performed with oleic acid by adding 30 µL of degassed oleic acid (CAS# 112-80-1, Aldrich, technical grade, 90%, cat. no. 364525-1L) to each tube followed by ~1 min of vigorous manual shaking. The nanocrystals were then precipitated by adding ~0.5 mL of acetonitrile to each tube. The tubes were then centrifuged once again and the supernatant was discarded. The washing procedure with toluene, oleic acid, and acetonitrile was repeated once more and then the nanocrystals were dried under vacuum for an hour.

Specifications of chemicals, instruments, and software

The excitation of the samples at 488 and 457.9 nm was done by an Ion Laser Technology Model 5500ASL-00 Ar⁺ laser producing ~70 mW at 488 nm and ~17 mW at 457.9 nm and

equipped with an intracavity Littrow prism to tune the wavelength. The laser was reflected off two New Focus flat enhanced silver mirrors and focused through a Thor Labs 1" diameter 10 cm focal length lens onto the sample. The setup is presented in Figure 6. The sample was present as a solution in a 1x1 cm quartz cuvette.

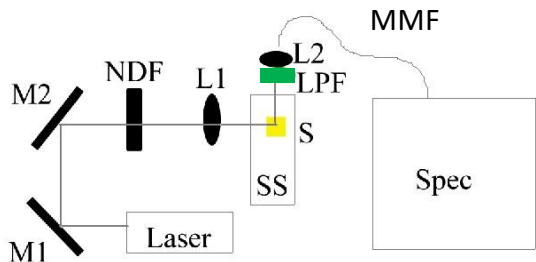


Figure 6: Raman setup for 488 and 457.9 nm excitation. M1- Mirror 1, M2- Mirror 2, NDF- Neutral Density Filter, L1- Lens 1 (focal length = 10 cm), S- Sample, SS- Sample Stage, LPF- Longpass Filter, L2- Lens 2, MMF- multimode fiber, Spec- Spectrometer.

Light scattering of samples excited by 488 nm and 457.9 nm excitation wavelengths was passed through an Omega Optical 490 nm or 460 nm longpass filter followed by an objective lens to focus the light onto a multimode fiber and collected on an Acton SpectraPro 300i 0.300 m Imaging Triple Grating Monochromator equipped with a Roper Scientific liquid nitrogen cooled back-illuminated CCD. The grating selected for all data collected here had a groove density of 1800 mm^{-1} . The data from the instrument was processed with Winspec/32 running on Windows XP Professional Version 2002 Service Pack 3.

All data for 532 nm excitation was collected with a Horiba Scientific Jobin Yvon XploRa with Olympus MPlan N 10x0.25 objective selected. The data from the instrument was processed with LabSpec 5 software. The sample was present as a solution in a Vitrocom 0.5 x 0.1 mm square borosilicate glass capillary.

UV-Vis data was collected on a Cary 5000 UV-Vis-NIR Spectrophotometer in a 1x1 cm quartz cuvette. ^1H NMR and ^{13}C NMR data were collected on a Bruker 300 MHz instrument. IR absorption data was collected on a Nicolet Avatar FTIR instrument with the sample present as a 3-5 μL drop of solution between two 1" polished KBr discs. Note: Anytime a S-OIAM solution was prepared for the study, it was prepared inside inert atmosphere with purified OIAM and powdered sulfur.

Results and Discussion

It was observed that technical grade 70% oleylamine (CAS# 112-90-3, Aldrich, technical grade, 70%, cat. no. O7805-500G) and oleylamine $\geq 98\%$ primary amine (CAS# 112-90-3, Aldrich, $\geq 98\%$ (primary amine)) come shipped with impurities that cause secondary radiation, rendering it unsuitable for Raman spectroscopy (red and green spectra in Figure 7). These impurities are photoluminescent when excited by 532-457.9 nm light and possibly a larger range of wavelengths. As stated above in the Introduction section, this is a common problem in resonance Raman spectroscopy. The multistep purification method described in the Methods section leads to the removal of these photoluminescent impurities and thus the ability to study OIAM and solutions of OIAM by Raman spectroscopy at excitation wavelengths of 488 and 532 nm. Figure 7 shows the Raman spectrum of samples of purified and unpurified OIAM, as well as OIAM that had been

purified by vacuum distillation only. From Figure 7 it is estimated that the impurity emission is reduced by a factor of roughly 25,000 after the purification is performed.

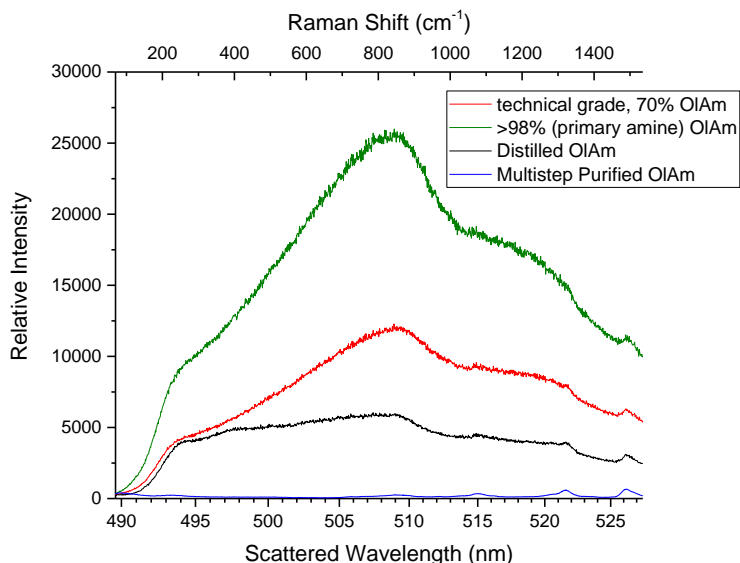


Figure 7: Secondary radiation from various samples of oleylamine (OlAm). Decreasing the impurity emission by a factor of ~25000 by a multistep purification method allows a resolved Raman spectrum of oleylamine to be obtained. All spectra were collected for 30 seconds, but normalized so that the Raman peak near 526 nm had the same height above the photoluminescent background.

The photoluminescent impurities are still observable and obscure the Raman spectrum when the purified OlAm is excited by 457.9 nm light (Figure 8a). This is unfortunate because the resonance Raman effect should start to manifest for the S_2^- , S_4^{2-} and S_6^{2-} species at this wavelength and shorter wavelengths. Therefore, it is difficult to study these polysulfide species by resonance Raman even with the purified OlAm. It is possible these impurities could be further removed by performing a OlAm purification twice over to obtain a clean Raman spectrum at 457.9 nm, although that was not attempted in this study. These photoluminescent impurities were unable to be identified and are further discussed below.

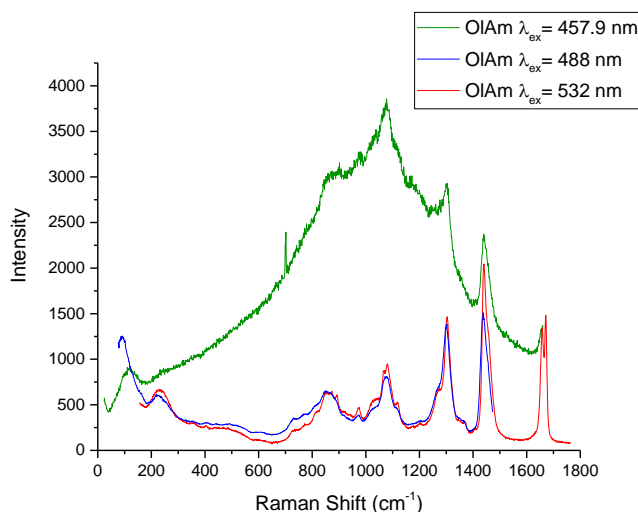


Figure 8a: Raman spectrum of multistep purified oleylamine (OlAm) at different excitation wavelengths, λ_{ex} . A large increase in secondary radiation appears when the sample is excited by 457.9 nm and obscures the Raman peaks. The sharp feature at ~650 cm^{-1} is likely due to a collision of a cosmic ray with the CCD.

Most of the expected Raman active modes for the OIAM molecule are observable in the Raman spectrum with 488 and 532 nm excitation wavelengths (Figure 8b) and the assignments are tabulated in Table 2 (within the wavelength range collected). The NH₂ scissor mode was not observed. This is consistent with the report of Lin-Vien et al. that this is a “very weak” (vw) peak. The best candidate for the peak at 1670 cm⁻¹ is the trans-dialkyl C=C assignment, suggesting a mixture of the cis and trans isomers. This hypothesis has not yet been tested by other methods. Additionally, the peak at 1442 cm⁻¹ is probably two separate peaks from the CH₂ scissor and asymmetric bending modes which show up in very close regions according to Lin-Vien et. al.³⁶ The peak center at ~850 cm⁻¹ also may be multiple peaks composed of the C-C stretch and R-NH₂ wag modes. The vibrational mode responsible for the peak center at 223 cm⁻¹ is unknown.

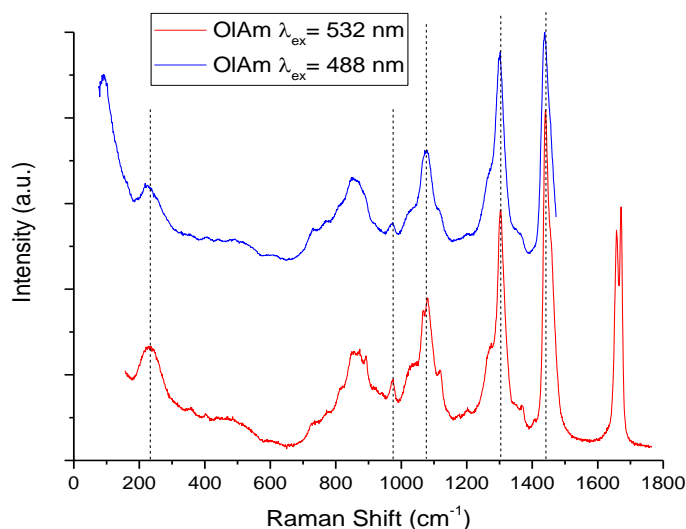


Figure 8b: Raman spectra of multistep purified oleylamine (OIAM) excited by 488 nm (blue) and 532 nm (red). The same spectra as in Figure 8a are shown although the position of the 488 nm excited spectrum is shifted vertically above the 532 nm excited samples for easier comparison of the peak maxima. The vertical lines show that the peaks line up within the instrumental uncertainty of a few wavenumbers when plotted as Raman shifts, thus proving that these peaks are due to Raman scattering and not relaxed photoluminescence (for relaxed photoluminescence, the emitted frequencies would coincide). The y-axis has arbitrary units (a.u.) of intensity.

Peak Position (cm ⁻¹)	1670	1658	1442	1298	1275	1075	971	851 ± 20	223
Peak Intensity	s	s	vs	s	s	m	vw	m	m
Assignment	trans-dialkyl C=C	cis-dialkyl C=C	CH ₂ scissor and asym.bend	CH ₂ twist	Cis CH sym. Rock	C-N stretch	Trans C-H wag	C-C stretch and R-NH ₂ wag	?
Peak Position from Reference 36	1676-1665	1662-1631	1475-1445 and 1470-1440	1305-1295	1270-1250	1090-1040	980-965	900-800 and 854-778	
Intensity from Reference 36	vs	vs	Both s-m	s	s	s-m	vw	s-m and s, br	

Table 2: Assignments for oleylamine Raman spectrum shown in Figure 9b. “vs”- very strong, “s”- strong, “s-m”- strong-medium, “m” – medium, “vw”- very weak, “br”- broad.

Having obtained a clean Raman spectrum of OIAM, the study was moved forward by adding elemental sulfur to the purified OIAM and obtaining a Raman spectrum of this solution at 488 nm excitation at room temperature. Studying solutions of S-OIAM heated to 120 °C was of interest because that is the temperature at which our standard PbS nanocrystal synthesis procedure (based on Weidman et al.) takes place.¹⁰ The Raman spectrum is reasonably well resolved when the solution is kept at room temperature, but upon heating the S-OIAM solution to 120 °C for 20 minutes, the spectrum shows signs of photoluminescence and is no longer well resolved. Careful inspection of the Raman spectrum baseline in the S-OIAM solutions shows the possibility that even at room temperature there may be formation of photoluminescent species which increase in concentration upon further heating. For this reason, a “sweet spot” of sorts was found at 40 °C, at which point the Raman spectrum is still well resolved and PbS nanocrystal synthesis can still be performed. As a control, to ensure the photoluminescent species were due to the presence of sulfur and not due to the amine itself, we heated the purified OIAM to 120 °C for 20 minutes (Figure 9).

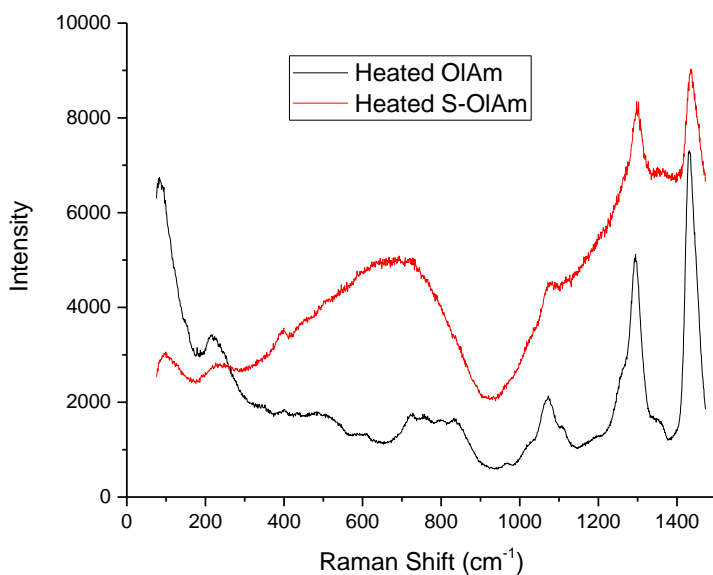


Figure 9: Once S-OIAM is heated, the Raman spectrum is no longer well resolved. Both solutions were heated to 120 °C for 20 minutes.

The heated OIAM alone (without sulfur) was still able to produce a resolved Raman spectrum after heating. It is unknown why the peak feature near 800 cm⁻¹ was “flattened out”, but a Raman spectrum of unheated OIAM taken on the same day showed the same feature. The formation of photoluminescent species upon heating S-OIAM agrees with McPhail and Weiss’ observation that fluorescent species form when sulfur is heated in ODE.³² It should be noted that the sample from which the black spectrum in Figure 9 was taken was a sample of oleylamine that was stored in a foil-wrapped glass vial capped with a Teflon-lined screw cap under air at 4 °C for a period of ~1 month. It is possible that photochemical reactions may have occurred if the sample was not wrapped in foil and/or oxidation may have occurred to produce impurities if the vial was not capped with a Teflon-lined cap. A control experiment to test for photochemical or oxidation products was not performed.

Studies of solution of sulfur in octylamine have shown that the sulfur peaks in the Raman spectrum change over time.³⁴ Additionally, studies by Daly and Brown had previously shown that the concentrations of polysulfides in amines change over time.³³ For purified OIAM that gave clean Raman spectra, it was unknown whether the same phenomenon would be observed in a solution of S-OIAM. This was indeed the case as evidenced by the Raman spectrum and UV-vis absorbance spectrum of sulfur oleylamine solution changing over time (Figures 10a,10b, 11 and Tables 3,4).

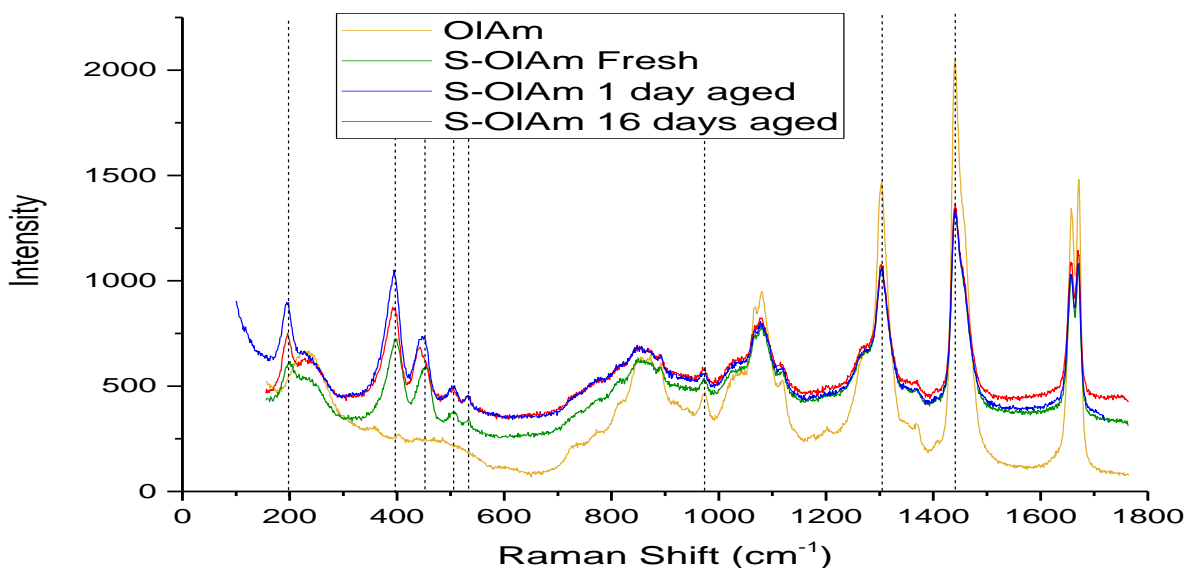


Figure 10a: Raman spectra of samples of sulfur in multistep purified oleylamine (S-OIAM) taken at various times after the sample was prepared. The “OIAM”, “S-OIAM Fresh”, and “S-OIAM 16 days aged” data were collected on different samples. The “S-OIAM Fresh” and “S-OIAM 1 day aged” data were collected from the same sample. The dashed vertical lines show that some peaks stay in the same position, whereas the peaks at $\sim 450\text{ cm}^{-1}$ appear different over time. This may be due to the presence of a doublet at 450 cm^{-1} where one of the peaks increases in intensity as time increases and/or another peak decreases in intensity as time increases. All samples were prepared and kept under inert atmosphere.

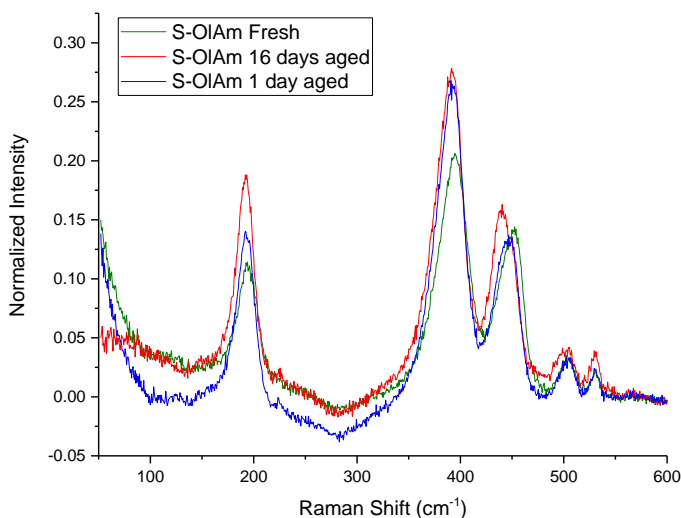


Figure 10b: Same as Figure 10a except collected with a 2400 grooves/mm grating instead of an 1800 grooves/mm grating and solvent subtracted.

Time (days)	Wavenumber (cm ⁻¹)						
pur. OlAm					223.4±0.4	866.4±2	969.7±0.2
S in OlAm							
0	393.4±2	447.4±2	503.2±0.8	529.0±0.4	196.4±2	854.4±2	967.4±0.2
1	391	444	502	529	193	856	969
48	389.5±0.4	442.3±0.3	499.7±0.8	529.6±0.3	193.6±0.4	857.0±0.3	968.0±0.2
16	389	441	499	528	193	856	969
30	389.6±0.3	441.5±0.5	499.1±4	529.8±0.6	193.1±0.4	856.2±0.9	967.5±0.3

Table 3: Quantitative results of data presented in Figure 10b. The error is presented as a 95% confidence interval. We took 3 spectra of each sample and rearranged the cells after each collection to obtain the data and error estimate. The first row shows the purified oleylamine solvent peaks so that possible background subtraction errors can be appreciated. The 1 day sample and 16 day sample were only taken once and this was on a different day than all the other spectra were taken, so no error is presented for them. All samples were different except for the 16 day and 30 day.

Species	S ₂ ⁻	S ₃ ⁻			S ₄ ²⁻	S ₆ ²⁻
UV-vis absorbance (nm)	400 ^a	620 ^c	600 ^d		440 ^h	440 ⁱ
Raman peaks (cm ⁻¹)	591 ^b	533 ^c	535 ^d	534 ^j (w)	193 ^j (vw)	453 ^q (m)
					397 ^j (vs)	495 ^q (w)
					438 ^j (s)	504 ^q (w)
					505 ^j (m)	
Ref	7,26	21	7	27,37	27,29,37	28,29

Table 4: Relevant literature values from Table 1 for easy comparison with Table 3. The relative intensities for the Raman peaks were added. "vs"-very strong, "s"-strong, "m"-medium, "w"-weak, "vw"-very weak.

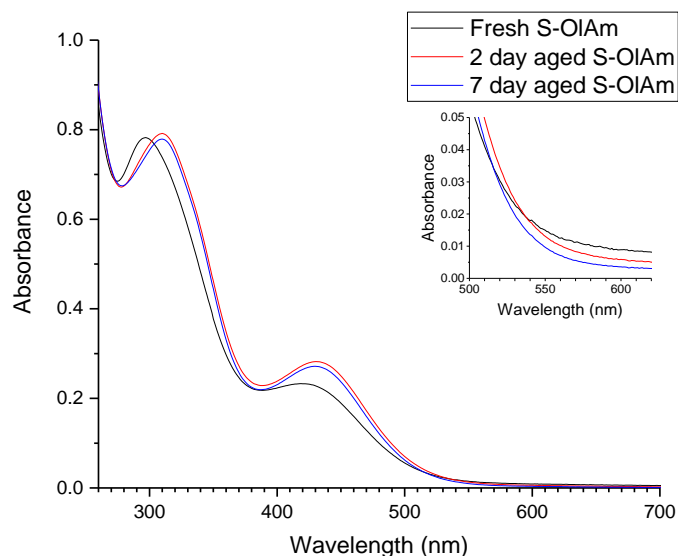


Figure 11: UV-vis spectra of sulfur in multistep purified oleylamine (S-OlAm) taken at various times after the sample had been prepared. The inset shows the region of 500-620 nm zoomed in. This is the region where the extinction coefficient of the aged and the fresh samples are the same. All samples were prepared and kept under inert atmosphere.

In the Raman data, a shift in the band near $\sim 450\text{ cm}^{-1}$ from the blue shoulder to the red shoulder, an increase in the intensity of the $\sim 193\text{ cm}^{-1}$ band, a red-shift of the ~ 400 and $\sim 500\text{ cm}^{-1}$ bands, and an increase in the intensity of the $\sim 535\text{ cm}^{-1}$ band in the 16 day sample is observed. Additionally, when the sample is excited at 488 nm, the $\sim 535\text{ cm}^{-1}$ band is not observed, whereas when the sample is excited at 532 nm, the $\sim 535\text{ cm}^{-1}$ band is observable. The band at $\sim 535\text{ cm}^{-1}$ is likely the S_3^- species which intensifies Raman scattering upon excitation at 532 nm vs. 488 nm due to the resonance Raman effect. I propose the band at $\sim 450\text{ cm}^{-1}$ consists of two very close lying peaks assigned to S_4^{2-} and S_6^{2-} . Daly and Brown have already proposed that the concentrations of S_3^- and S_4^{2-} increase over time in primary amines.³⁷ This proposition is consistent with the Raman data. In addition to this I propose the concentration of S_6^{2-} decreases over time. It should be noted here that FTIR absorbance of fresh S-OIAM was obtained and one peak at 501 cm^{-1} was observed. This is consistent with an assignment of S_6^{2-} (IR peak of 502 cm^{-1}).²⁸ No FTIR of aged S-OIAM was obtained. If this proposition is indeed true, then this leads to the question of where the extra sulfur atoms run off to.

Thomson et al. has suggested that the species responsible for metal sulfide nanocrystal synthesis is H_2S .³¹ To test the hypothesis that H_2S is responsible for QD nucleation, a synthesis of PbS QDs at $40\text{ }^\circ\text{C}$ was performed, along with a qualitative test for determining whether H_2S evolves from the S-OIAM precursor at these temperatures. Figure 12 shows that it is possible to obtain PbS QDs with one single peak when the synthesis is performed at $40\text{ }^\circ\text{C}$. To perform the qualitative test for H_2S evolution, an apparatus wherein N_2 gas was bubbled through a solution of S-OIAM and the outlet went into a solution of lead nitrate was assembled. H_2S will react with lead nitrate to a great extent to form PbS as a precipitate ($K_{\text{spa}} = 3 \times 10^{-7}$)³⁸ at which point the solution will begin to turn brown. From this apparatus, it was observed that at these low temperatures ($40\text{ }^\circ\text{C}$) hydrogen sulfide is not produced to any appreciable extent. More specifically, no color change was observed (by naked eye observation) while the S-OIAM was at $40\text{ }^\circ\text{C}$ for 10 minutes. After these 10 minutes, the temperature was ramped to $55\text{ }^\circ\text{C}$. After 20 minutes at $55\text{ }^\circ\text{C}$ there was a very slight hint of brown. The heat was then ramped to $70\text{ }^\circ\text{C}$ and an obvious color change to brown was observed within 10 minutes (see Appendix, Figure A1).

To test whether the aged solutions of S-OIAM gave different QDs, a synthesis of PbS QDs with freshly prepared (<1 hour aged) S-OIAM and another synthesis with 2 days aged S-OIAM was performed. The syntheses gave dramatically different results. In the PbS QD absorption spectrum a single peak was observed when the precursor was the fresh S-OIAM (red, Figure 12). In the PbS QD absorption spectrum with the aged S-OIAM two unresolved peaks were observed (black, Figure 12). This shows that QD synthesis should be performed with freshly prepared precursor solution to obtain more desirable properties of QDs (i.e. narrower size distribution). It should be noted here that the PbS synthesis was performed under oxygen-free conditions. It is possible that if the synthesis were to be performed under conditions where oxygen is present that different results may be obtained.

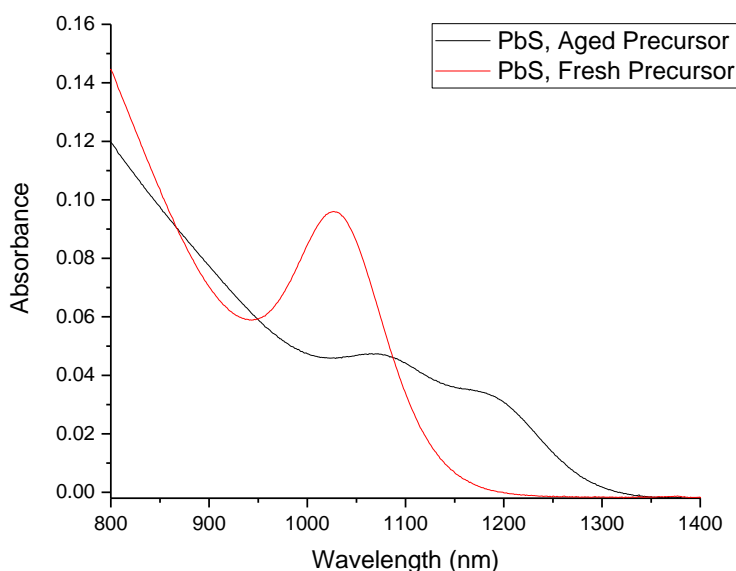


Figure 12: PbS QDs synthesized with sulfur in multistep purified oleylamine precursor that had been aged for different times. The “Aged Precursor” had been aged for 2 days before being used in the synthesis and the “Fresh Precursor” had been used within 1 hour after preparation.

Optimally, to mimic the most commonly used metal sulfide QD synthesis procedures, S-OIAM solutions heated to high temperatures would be of most interest in this study. However, as stated above, photoluminescent products obscure the Raman spectrum after the solution has been heated, which agrees with McPhail and Weiss’ observation that fluorescent species form when sulfur is heated in ODE. McPhail and Weiss also observed that when sulfur was heated in ODE for 5 min vs. 90 minutes the peaks in the chemical shift region of 3.7 to 2.5 ppm grew. ^1H NMR and ^{13}C NMR data were collected on samples of S-OIAM heated to different temperatures. In the 3.7 to 2.5 ppm region in the ^1H NMR spectra of S-OIAM solution heated to 120 °C for 2 hours, small peaks were observed. These peaks grew when the same experiment was performed at 180 °C (Figure 13).

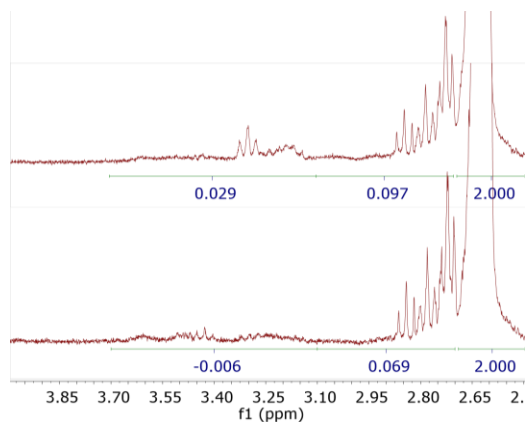


Figure 13: ^1H NMR region of 4.0 to 2.5 ppm. The top spectrum shows the solution heated to 180 °C for 2 hours and the bottom spectrum shows the solution heated to 120 °C for 2 hours. The numbers below the spectra are the integrated values of that region. Both are in CD_2Cl_2 and referenced with the middle peak of the CH_2Cl_2 triplet at 5.32 ppm. The region from 2.69 to 2.44 ppm (alpha hydrogen position) was normalized to 2.000 in both spectra. Both spectra are of 5.95 mg/mL S-OIAM dissolved in CD_2Cl_2 .

This may be evidence of sulfur reacting with the double bond of oleylamine because McPhail and Weiss assign the peaks in the region of Figure 13 to organosulfur products of reactions of sulfur with 1-ODE, a molecule with no amine functional group present. The species present in the heated solution that were not present in the unheated solution were not identified. McPhail and Weiss assign three types of products to the peaks that grow upon further heating in this region. The first is an attachment of a sulfur chain to the terminal carbon and migration of the double bond to the adjacent carbon. Second, is loss of the double bond by attachment of hydrogen to one carbon and sulfur to the other (Figure 4b). Third, is loss of the double bond by the attachment of a sulfur chain to the terminal carbon and attachment of another ODE molecule to the other carbon.³² Evidence for products of the second or third type is not observed because if this was the case a decrease in the vinylic (H attached to C of double bond) signal as compared to the methyl proton (relatively unreactive) signal would be expected and this ratio was not observed to change from the data. Thus, the data is consistent only with the previously proposed organosulfur products shown in Figure 14 when sulfur is heated in OIAM.

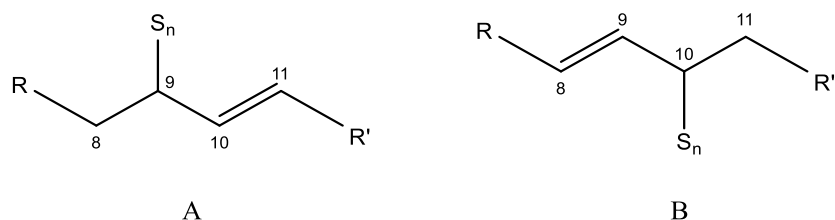


Figure 14: Possible products formed when S-OIAM is heated. The numbers show the carbon number on the oleylamine molecule (double bond is normally between 9 and 10). “R” represents $\text{NH}_2(\text{CH}_2)_7-$ and “R’ ” represents $-(\text{CH}_2)_6\text{CH}_3$. S_n represents a sulfur chain of n atoms.

Additionally, Thomson et. al. state that heated sulfur in octylamine produces octanethioamide based on ^{13}C NMR resonance at 204 ppm.³¹ No peaks from 140-220 ppm in the ^{13}C NMR data of S-OIAM heated to 120 °C for 20 minutes were observed in our data and therefore oleylthioamide formation likely does not occur under these conditions. A possible reason for the differences between sulfur in octylamine vs. sulfur in oleylamine is the presence of the double bond in oleylamine. Chemistry may be occurring at the double bond in OIAM which is more favorable than similar chemistry to octylamine occurring at the amine, thus there may be products such as those in Figure 14, instead of oleylthioamide, when sulfur is heated in OIAM.

Although the impurities present in the OIAM were not the focus of the study, a mass spectrum of both purified and unpurified oleylammonium chloride salt was obtained.¹¹ From the mass spectra, there is reason to postulate the photoluminescent species may contain “NO” or “NO₂” in the molecular formula, although the connectivity of these atoms is uncertain. A summary of the mass spectrum is shown in Figure 15.

$m/z, z = 1$	counts, norm. crude	counts, norm. purified	molecular formula	comments
214.25376	0.02	0.01	C ₁₄ H ₃₂ N	
240.26947	0.06	0.03	C ₁₆ H ₃₄ N	
242.28488	0.05	0.09	C ₁₆ H ₃₆ N	
254.28523	0.01	0.01	C ₁₇ H ₃₆ N	
256.30033	0.01	0.02	C ₁₇ H ₃₈ N	
266.28497	0.13	0.07	C ₁₈ H ₃₆ N	
268.3006	1	1	C₁₈H₃₈N	
280.26415	0.03	<0.001	C ₁₈ H ₃₄ NO	
282.27698	0.16	<0.001	C ₁₈ H ₃₆ NO	
282.32048	<0.01	<0.01	C ₁₉ H ₄₀ N	
296.25849	~0.01	<0.001	C ₁₈ H ₃₄ NO ₂	
296.33158	~0.01	~0.02	C ₂₀ H ₄₂ N	
300.28996	0.02	<0.001	C ₁₈ H ₃₈ NO ₂	
313.17235	0.03	<0.001	C ₁₈ H ₃₉ NCO ₂	(?) or artifact

Figure 15: A summary of the differences between mass spectra of purified oleylamine and unpurified. Note that the largest change is in the species with “NO” or “NO₂” in the molecular formula.

Conclusion

A solution of sulfur dissolved in oleylamine is an important precursor for lead sulfide nanocrystal synthesis. A solution of this kind was studied by Raman, UV-vis absorbance, IR absorbance, and ¹H and ¹³C NMR spectroscopy. This study has shown that it is possible to study solutions of this kind by Raman spectroscopy if one purifies the oleylamine according to the method used here to decrease the amount of impurity photoluminescence. Having a purified oleylamine sample, the first Raman spectrum of this compound was obtained. Furthermore, a Raman spectrum of sulfur dissolved in purified oleylamine was obtained, showing distinctive peaks due to sulfur species. This solution was studied as a function of time and changes in the Raman and UV-Vis spectra were observed. The observations are consistent with the concentration of the S₄²⁻ polysulfide species increasing over time and the concentration of S₆²⁻ decreasing. Additionally, the observations are consistent with the presence of S₃⁻. PbS nanocrystal synthesis performed on fresh and aged S-OIAM solutions show that a narrower size distribution results when the fresh precursor is used. Solutions of this kind are unable to be studied by Raman at high temperatures (usual nanocrystal synthesis temperatures) because photoluminescent compounds are formed (or concentrations of these species dramatically increase) once the solution is heated to 120 °C. This photoluminescence may be due to products from reaction of sulfur at the double bond of oleylamine or to contaminants of uncertain origin that contain “NO” or “NO₂” in the molecular formula detected by mass spectroscopy.

Acknowledgements

I thank Dr. David Jonas for advising, helping me plan and prepare my thesis, accepting me into his research group, and making the lab wheelchair accessible, Dr. Robert Parson for help with planning my thesis timeline, Dmitry Baranov for assistance with my experiments and his guidance, Curtis Beimborn and Dr. Mathias Weber for use of their 532 nm Raman instrument, and Jisu Ryu for helping me learn programming that has been of use in making this work.

References

- (1) Farmer, E. H.; Shipley, F. W. *J. Chem. Soc. Resumed* **1947**, 1519–1532.
- (2) Moore, C. G.; Saville, R. W. *J. Chem. Soc. Resumed* **1954**, 2089–2094.
- (3) Moore, C. G.; Saville, R. W. *J. Chem. Soc. Resumed* **1954**, 2082–2089.
- (4) Scott, W.; Bedford, C. W. *Ind. Eng. Chem.* **1921**, *13* (2), 125–128.
- (5) Davis, R. E.; Nakshbendi, H. F. *J. Am. Chem. Soc.* **1962**, *84* (11), 2085–2090.
- (6) Clark, R.; Franks, M. *Chem. Phys. Lett.* **1975**, *34* (1), 69–72.
- (7) Clark, R. J.; Cobbold, D. G. *Inorg. Chem.* **1978**, *17* (11), 3169–3174.
- (8) Clark, R. J.; Dines, T. J.; Kurmoo, M. *Inorg. Chem.* **1983**, *22* (19), 2266–2772.
- (9) Mourdikoudis, S.; Liz-Marzán, L. M. *Chem. Mater.* **2013**, *25* (9), 1465–1476.
- (10) Weidman, M. C.; Beck, M. E.; Hoffman, R. S.; Prins, F.; Tisdale, W. A. *ACS Nano* **2014**, *8* (6), 6363–6371.
- (11) Baranov, D.; Jonas, D.; Lynch, M. Unpublished data, 2017.
- (12) Voronkov, M. G.; Vyazankin, N. S.; Deryagina, E. N.; Nakhmanovich, A. S.; Usov, V. A. *Reactions of Sulfur with Organic Compounds*; Plenum Publishing Corporation, 1987.
- (13) Hodgson, W. G.; Buckler, S. A.; Peters, G. *J. Am. Chem. Soc.* **1963**, *85* (5), 543–546.
- (14) MacColl, R.; Windwer, S. *J. Phys. Chem.* **1970**, *74* (6), 1261–1266.
- (15) Gobeltz, N.; Ledé, B.; Raulin, K.; Demortier, A.; Lelieur, J.-P. *Microporous Mesoporous Mater.* **2011**, *141* (1–3), 214–221.
- (16) El Jaroudi, O.; Picquenard, E.; Demortier, A.; Lelieur, J.-P.; Corset, J. *Inorg. Chem.* **2000**, *39* (12), 2593–2603.
- (17) Seel, F.; Guttler, H. J. *Angew. Chem.-Int. Ed. Engl.* **1973**, *12* (5), 420–421.
- (18) Seel, F.; Guttler, H. J.; Simon, G.; Wieckowski, A. *Pue Appl Chem* **1977**, *49*, 45–54.
- (19) Chivers, T.; Drummond, I. *J. Chem. Soc. Dalton Trans.* **1974**, No. 6, 631–633.
- (20) Chivers, T.; Drummond, I. *Chem. Soc. Rev.* **1973**, *2* (2), 233–248.
- (21) Chivers, T.; Drummond, I. *Inorg. Chem.* **1972**, *11* (10), 2525–2527.
- (22) Wild, M.; O'Neill, L.; Zhang, T.; Purkayastha, R.; Minton, G.; Marinescu, M.; Offer, G. J. *Energy Env. Sci* **2015**, *8* (12), 3477–3494.
- (23) Vandenabeele, P. *Practical Raman spectroscopy: an introduction*; John Wiley & Sons, Ltd: Chichester, West Sussex, United Kingdom, 2013.
- (24) Lakowicz, J. R. *Principles of Fluorescence Spectroscopy*; Springer Science & Business Media, 2007.
- (25) Michl, J.; Thulstrup, E. W. *Spectroscopy with Polarized Light*; VCH Publishers Inc., 1986.
- (26) Sawicki, C. A.; Fitchen, D. B. *Chem. Phys. Lett.* **1976**, *40* (3), 420–422.
- (27) Daly, F. P.; Brown, C. W. *J. Phys. Chem.* **1976**, *80* (5), 475–480.
- (28) Janz, G. J.; Coutts, J. W.; Downey Jr, J. R.; Roduner, E. *Inorg. Chem.* **1976**, *15* (8), 1755–1759.

- (29) Manan, N. S. A.; Aldous, L.; Alias, Y.; Murray, P.; Yellowlees, L. J.; Lagunas, M. C.; Hardacre, C. *J. Phys. Chem. B* **2011**, *115* (47), 13873–13879.
- (30) Pryor, W. *Mechanisms of Sulfur Reactions*; McGraw-Hill, 1962.
- (31) Thomson, J. W.; Nagashima, K.; Macdonald, P. M.; Ozin, G. A. *J. Am. Chem. Soc.* **2011**, *133* (13), 5036–5041.
- (32) McPhail, M. R.; Weiss, E. A. *Chem. Mater.* **2014**, *26* (11), 3377–3384.
- (33) Daly, F. P.; Brown, C. W. *J. Phys. Chem.* **1975**, *79* (4), 350–354.
- (34) Baranov, D.; Jonas, D. Unpublished data, 2016.
- (35) Scott Gibson. Process for the preparation of saturated or unsaturated primary fatty amines. EP 1746084 B1, July 22, 2005.
- (36) Lin-Vien, D.; Colthup, N.; Fateley, W. G.; Grasselli, J. G. *The Handbook of Infrared and Raman Characteristic Frequencies of Organic Molecules*; Academic Press, 1991.
- (37) Daly, F.; Brown, C. *J. Phys. Chem.* **1973**, *77* (15), 1859–1861.
- (38) W. M. Haynes. *CRC Handbook of Physics and Chemistry*, 97th ed.; CRC Press/Taylor & Francis: Boca Raton, FL.

Appendix

Oleylamine Purification Procedure:

Note: Purification of commercial oleylamine through conversion to oleylammonium chloride and back to oleylamine was adopted from the following reference with modifications (relative amounts of solvents were scaled down by a factor of 3/4): Gibson, Scott. "Process for the preparation of saturated or unsaturated primary fatty amines." U.S. Patent No. 7,705,186. 27 Apr. 2010.

Reagents: Oleylamine (CAS# 112-90-3, Aldrich, $\geq 98\%$ (primary amine), cat. no. HT-OA100-1.5KG), ethyl ether (BDH1121-1LPC, stabilized with 1 ppm of BHT, ACS grade, 1L, BDH), acetonitrile (A21-1, Certified ACS, 1L, Fisher Scientific), hydrochloric acid (H613-05, 36.5%-38%, Meets ACS Reagent Chemical Requirements, Macron Chemicals), sodium hydroxide (S318-500, Certified ACS, Fisher Scientific), deionized water (Milli-Q™ grade), sodium sulfate (S421-500, anhydrous, Certified ACS, Fisher Scientific).

Glassware and equipment: a magnetic stirring & heating plate and a stirring bar, 500 ml single-neck round bottom flask, 1000 ml Erlenmeyer flask, 1000 ml Erlenmeyer flask with a vacuum adapter, porcelain Buchner funnel 90 mm diameter, Whatman® filter paper circles (grade 1, 90 mm diameter), glass rod, 500 ml separatory funnel, 100 ml and 10 ml graduated cylinders, Pasteur pipettes and bulbs, Hengar boiling chips (High purity, white, amphoteric alundum granules), sand bath, temperature controller.

50 ml of oleylamine (0.15 moles, clear pale yellow liquid) was mixed with 160 ml of ethyl ether in 500 ml round bottom flask. Under stirring, 15.5 ml (~1.2 equiv. of HCl) of concentrated hydrochloric acid was added to it dropwise using Pasteur pipette over 10 minutes. Next, 1000 ml Erlenmeyer flask was charged with 500 ml of acetonitrile, and oleylammonium chloride-ether solution was added to it dropwise under stirring forming white cloudy precipitate. The resulting mixture kept in ice bath for 30 minutes, filtered on air and rinsed four times with 100 ml portions of acetonitrile. The snowy white fluffy solid was transferred to 500 ml round bottom flask and dried under vacuum for 30 minutes. In the meantime, 12.3 grams of sodium hydroxide (~2 equiv.) were dissolved in 150 ml of deionized water. 200 ml of ethyl ether were added to dried solid of oleylammonium chloride forming white slurry, equipped with magnetic stirring bar and placed on magnetic stirring plate. Next, sodium hydroxide solution was added to the oleylammonium chloride slurry in ethyl ether in small portions. Upon addition of sodium hydroxide white slurry gradually changed appearance to light yellow two phase mixture (ether solution of oleylamine on top, aqueous solution of sodium chloride and hydroxide on the bottom). After all sodium hydroxide was added, two phase mixture was transferred to a separatory funnel, shaken a couple of times, after which organic and aqueous phases were let to separate. Aqueous phase was discarded and organic phase was washed four times with 50 ml of deionized water. After the last wash, organic phase was transferred to 500 ml round bottom flask and dried with anhydrous sodium sulfate overnight. Next day, excess ether solvent was removed under nitrogen and residual oleylamine distilled under vacuum. During the distillation, very first fraction (~3/4 of ml) was collected in a

separate flask to not contaminate final product. Distilled oleylamine, a colorless liquid, was either stored at 4 °C in foil-wrapped glass vials capped with Teflon-lined screw caps under normal atmospheric air or stored in the same vials at ~34 °C under N₂ atmosphere.

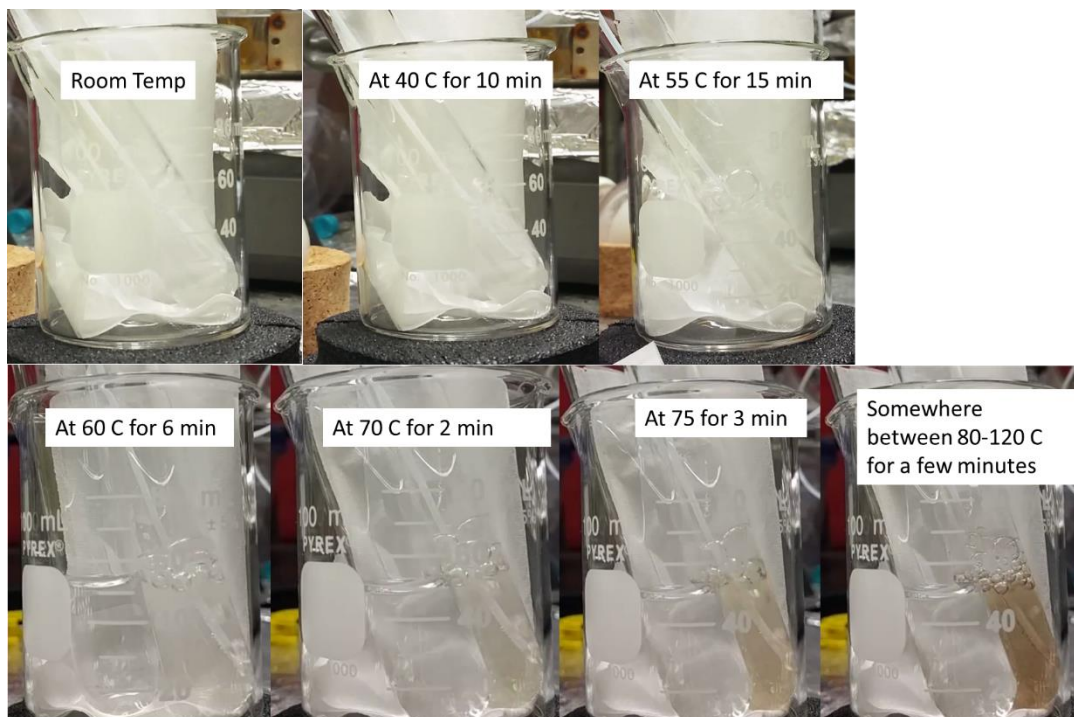


Figure A1: Progression of pictures showing a test tube filled with lead nitrate. The first picture in the second row is when another test tube of water was added to compare the colors of the two solutions more easily.

Distilled OIA (cm ⁻¹)		Sulfur in Distilled OIA (cm ⁻¹)		Assignment	Ref
		501	w	S-S stretch	pg 231-232 Lin-Vien
723	m	723	mw	cis-CH wag, (CH ₂) _n in phase rock	pg 74, 11 Lin-Vien
800	m	800	w	NH ₂ wagging	pg 156 Lin-Vien
966	m	966	m	trans-CH wag	pg 74 Lin-Vien
1073	w	1073	vw	CN stretching	pg 156 Lin-Vien
1091	w	1091	vw	CN stretch	pg 156 Lin-Vien
1262	w	1262	w	cis-CH sym. Rock	pg 11 Lin-Vien
1306	m w	1306	mw	trans-CH sym. Rock	pg 11 Lin-Vien
1352	m	1352	m	? -NO ₂	pg 181 Lin-Vien
1359	m	1359	m	? -NO ₂	pg 181 Lin-Vien
1378	m	1378	m	CH ₃ sym. Bend	pg 11 Lin-Vien
1402	w	1402	w	?	
1437	vs	1437	vs	CH ₂ scissor	pg 11 Lin-Vien
1457	s	1457	s	CH ₂ scissor	pg 11 Lin-Vien
1466	s	1466	s	CH ₃ asym. Bend	pg 11 Lin-Vien
		1589	m	antisymmetric NH ₃ + deformation	pg 173 Lin-Vien
1619	m	1619	w	NH ₂ scissor	pg 156 Lin-Vien
1652	w	1652	w	cis C=C stretch	pg 74 Lin-Vien
2033	vw	2033	m	? C≡N	pg 106 Lin-Vien
2170	vw	2170	m	? C≡N	pg 106 Lin-Vien
		2528	m	? S-H	pg 226 Lin-Vien
2680	m	2680	m	?	
2853	vs	2853	vs	sym. CH ₂ stretch	pg 11 Lin-Vien
2870	s	2870	s	sym. CH ₃ stretch	pg 11 Lin-Vien
2923	vs	2923	vs	antisym. CH ₂ stretch	pg 11 Lin-Vien
2954	vs	2954	vs	antisym. CH ₃ stretch	pg 11 Lin-Vien
3004	m	3004	m	cis C=C-H stretch	pg 74 Lin-Vien
		3152	vw		
3186	w			NH ₂ symmetric stretch	pg 160 Lin-Vien
		3259	w		
3297	w			NH ₂ symmetric stretch	pg 160 Lin-Vien
		3350	w		
3374	w			NH ₂ asymmetric stretch	pg 160 Lin-Vien
3678	vw				

Table A1: IR data of OIAm and S-OIAm solutions taken on the same day as preparation.